ELSEVIER

Nuclear Instruments and Methods in Physics Research A 428 (1999) 551–555

NUCLEAR INSTRUMENTS & METHODS IN PHYSICS RESEARCH Section A

www.elsevier.nl/locate/nima

Data analysis for inelastic nuclear resonant absorption experiments

M.Y. Hu[a,b,*], W. Sturhahn[a], T.S. Toellner[a], P.M. Hession[a,c], J.P. Sutter[a,c], E.E. Alp[a]

[a]*Advanced Photon Source, Argonne National Laboratory, 431/D002, Argonne, IL 60439, USA*
[b]*Northwestern University, Dept. of Physics and Astronomy, Evanston, IL 60208, USA*
[c]*Purdue University, Dept. of Physics, West Lafayette, IN 47907, USA*

Received 3 December 1997; received in revised form 10 December 1998

Abstract

Inelastic nuclear resonant absorption method has been applied to study lattice dynamics. The data evaluation procedure for such experiments using synchrotron radiation is presented. Various moments of the measured spectra provide model-independent information on vibrational excitations, such as the recoilless fraction, the average kinetic energy per nucleus, and the average force constant. In addition, the partial phonon density of states is extracted assuming a harmonic lattice model. A measurement performed on α-iron is shown as an example. © 1999 Elsevier Science B.V. All rights reserved.

PACS: 63.20.Dj; 82.80.Ej; 07.85.Qe

Recently, inelastic nuclear resonant absorption of synchrotron radiation has been applied as a technique to study phonon excitations [1,2]. The further development of crystal optics with sub-meV energy resolution [3] and the high brightness of undulator sources at the third-generation synchrotron radiation facilities have made this technique a unique way to study vibrational dynamics in materials. Certain isotopes with low-lying nuclear levels can be resonantly excited by X-rays. Since the linewidth of the excited nuclear level is usually on the order of neV, X-rays with energy within this narrow energy bandwidth can excite nuclei recoilessly and this is the Mössbauer effect. X-rays with energy out of this narrow range can also excite the nuclei by involving phonons in the material. This inelastic excitation was predicted in the 1960s [4,5], and it provides information on the vibrational dynamics of the resonant nuclei. In contrast to the Mössbauer effect, where the recoilless excitations are studied, this inelastic approach exploits the energy transfer between X-rays and lattice. Because only a particular type of isotope can be resonantly excited by X-rays with energy close to its resonant energy, this method provides a way to study dynamics of selected atoms, i.e., nuclear resonant isotopes, in materials.

The resonant excitation, both elastic and inelastic, can be observed by detecting nuclear decay products, i.e., nuclear fluorescence, internal

* Corresponding author. Tel.: +1-630-252-0168; fax: +1-630-252-0161.

E-mail address: myhu@aps.anl.gov (M.Y. Hu)

PII: S0168-9002(99)00134-5

conversion electrons, and atomic fluorescence following internal conversion process. Synchrotron radiation is a pulsed X-ray source, and the pulse length is on the order of 100 ps at the third-generation source. On the other hand, excited nuclear level has a certain lifetime, so that its decay is delayed in time. When the nuclear resonant lifetime is much longer than the synchrotron pulse length, the nuclear resonant scattering process is distinguished from electronic scattering by counting signals only after the disappearance of the prompt radiation and electronic scattering. This leads to an enormous background suppression. Thus noise level is basically determined by the detector and the associated electronics, which can be suppressed well below the signal level in most cases [6]. The resulting high signal-to-noise ratio allows one to extract the higher-order multi-phonon contributions from the data.

The typical experimental setup for inelastic nuclear resonant absorption is shown in Fig. 1. The pre-monochromator reduces the X-ray energy bandwidth to a few eV and removes most of the heat load in the beam. The following high-resolution monochromator further reduces the energy bandwidth to meV or less, which is the experimental resolution needed to study phonon excitations. The detector is placed very close to the sample to collect as many nuclear decay signals as possible. In such an experimental arrangement, if the atomic K-fluorescence following the internal electron conversion is detected, the count rate observed [2] is,

$$I(\varepsilon) = I_0 d\rho \frac{\eta_K \alpha_K}{1+\alpha}\sigma(\varepsilon) \tag{1}$$

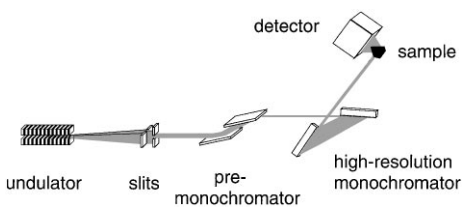

Fig. 1. The experimental setup of inelastic nuclear resonant absorption experiments.

where $\varepsilon = E - E_0$, E is the incident photon energy, E_0 is the nuclear resonant energy, I_0 is the incident photon flux, d is the detection efficiency, ρ is the effective area density of nuclei, η_K is the K-fluorescence yield, and α, α_K are the total and partial internal conversion coefficients. The nuclear resonant excitation cross section $\sigma(\varepsilon)$ is proportional to a Fourier transform, $S(\varepsilon, \boldsymbol{k})$, of the self-correlation function of the system [5]. This is because the inelastic resonant absorption is an incoherent process. In general, $S(\varepsilon, \boldsymbol{k})$, and thus the excitation cross section, also depends on the incident photon momentum $\boldsymbol{k}$. But for an isotropic lattice, this dependence can be dropped. So, we list all the basic equations with explicit $\boldsymbol{k}$ dependence and omit it later in data evaluation procedure:

$$\sigma(\varepsilon, \boldsymbol{k}) = N\frac{\pi}{2}\sigma_0 \Gamma S(\varepsilon, \boldsymbol{k}) \tag{2}$$

$$S(\varepsilon, \boldsymbol{k}) = \frac{1}{2\pi N}\int \mathrm{d}t\, \mathrm{e}^{-i\varepsilon t}\sum_i g_i \langle i| \times \sum_l \mathrm{e}^{-i\boldsymbol{k}\boldsymbol{r}_l(0)}\mathrm{e}^{i\boldsymbol{k}\boldsymbol{r}_l(t)}|i\rangle \tag{3}$$

where N is the number of resonant nuclei, σ_0 is the maximum resonant excitation cross section, and Γ is the natural linewidth of the resonance. For ^{57}Fe, $E_0 = 14.413$ keV, $\Gamma = 4.66$ neV, $\sigma_0 = 2.56 \times 10^{-18}$ cm^2. The g_i is the statistical weight factor of initial lattice state $|i\rangle$. The $\boldsymbol{r}_l$ is the position of the lth resonant nucleus. Here, $S(\varepsilon, \boldsymbol{k})$ is normalized to 1. It can be separated into elastic and inelastic contributions,

$$S(\varepsilon, \boldsymbol{k}) = f\delta(\varepsilon) + S'(\varepsilon, \boldsymbol{k}) \tag{4}$$

where f is the recoilless fraction. The separation of the inelastic part $S'(\varepsilon,\boldsymbol{k})$ is important in data evaluation procedure for reasons explained later.

For resonant absorption, there exist Lipkin's moment sum rules [7],

$$\int S(\varepsilon, \boldsymbol{k})(\varepsilon - E_R)\,\mathrm{d}\varepsilon = 0 \tag{5}$$

$$\int S(\varepsilon, \boldsymbol{k})(\varepsilon - E_R)^2\,\mathrm{d}\varepsilon = 4E_R\bar{T}_k \tag{6}$$

$$\int S(\varepsilon, \boldsymbol{k})(\varepsilon - E_R)^3\,\mathrm{d}\varepsilon = \frac{E_R}{m}\hbar^2\bar{F}_k \tag{7}$$

where $E_R = E^2/2mc^2$ is the recoil energy of the nucleus, m is the nuclear mass, $\bar{T}_k$ is the mean kinetic energy of the resonant nuclei in the $\boldsymbol{k}$ direction, and $\bar{F}_k$ is the mean force constant experienced by the resonant nuclei in the $\boldsymbol{k}$ direction. While the higher moments give us information on the vibrational dynamics of the sample, the first moment is employed to normalize the spectrum, as well as to determine the recoilless fraction, which is shown later.

The experimentally measured flux is not $I(\varepsilon)$ in Eq. (1), but rather the convolution of it with the normalized instrument resolution function $R(\varepsilon)$,

$$I_m(\varepsilon) = \int I(\varepsilon')R(\varepsilon - \varepsilon')\,d\varepsilon'. \tag{8}$$

And this leads to the following relations for the moments:

$$\langle I_m\rangle_0 = \langle I\rangle_0 \tag{9}$$

$$\langle I_m\rangle_1 = \langle I\rangle_1 + \langle I\rangle_0\langle R\rangle_1 \tag{10}$$

$$\langle I_m\rangle_2 = \langle I\rangle_2 + 2\langle I\rangle_1\langle R\rangle_1 + \langle I\rangle_0\langle R\rangle_2 \tag{11}$$

$$\langle I_m\rangle_3 = \langle I\rangle_3 + 3\langle I\rangle_2\langle R\rangle_1 + 3\langle I\rangle_1\langle R\rangle_2 + \langle I\rangle_0\langle R\rangle_3 \tag{12}$$

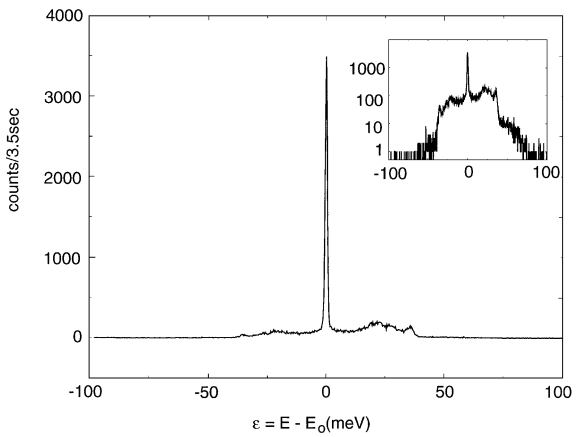

Fig. 2. The data taken on α-Fe foil, with energy resolution of 0.9 meV. The inset shows the same data on log scale.

where $\langle\ \rangle_n$ denotes the nth moment. Using these relations, the moments of $S(\varepsilon)$ can be calculated from those of $I_m(\varepsilon)$ and $R(\varepsilon)$, which are experimentally measured quantities.

In a recent experiment [3], an α-Fe foil is measured using the inelastic nuclear resonant absorption technique with an energy resolution of 0.9 meV. The sample is 95% enriched in ^{57}Fe, and is in polycrystalline form. One of the recorded spectra is shown in Fig. 2. The center spike is the elastic peak resulting from the recoilless nuclear resonant excitation. The inelastic excitation is clearly seen in the spectrum, which appears as wings to the elastic peak and extends to about 80 meV away from the peak. The low-energy side of the spectrum corresponds to phonon annihilation, the high-energy side phonon creation.

Usually, the elastic part of the function $S(\varepsilon)$ is appreciably larger than the inelastic part, $S(\varepsilon = 0) > S(\varepsilon \neq 0)$. In the case of enriched iron metal, the former is six orders of magnitude larger. So, the absorption of X-rays with the exact resonant energy is larger than the absorption involving lattice vibrations. This results in smaller penetration depth of the X-ray with exact resonant energy and less material contributing to the elastic peak. This elastic peak suppression is difficult to calculate and varies from experiment to experiment because it depends on the geometry of the setup. Instead of trying to figure out the suppression factor, we can remove the measured elastic peak and then replace it with the theoretical one, i.e., $f\delta(\varepsilon)$. Here the recoilless fraction acts like a fitting parameter, and is determined later by the first moment sum rule.

So, the first step in data evaluation is to fit the elastic peak in each data set with the instrument resolution function and then remove the peak from the spectrum. The instrument resolution function is measured by nuclear forward scattering, in which the elastic resonance is enhanced coherently in forward direction so that the nuclear resonance acts as an extremely fine probe to measure the energy bandwidth of the high-resolution monochromator. After the elastic peak has been removed in each individual data set, these spectra are combined into one data set to improve statistics. In Fig. 3 is shown the combined spectrum from five peak-removed data sets.

The next step is to normalize the spectrum and at the same time determine the recoilless fraction. Because part of the measured spectrum, the elastic peak, is suppressed by an unknown factor, it cannot be normalized by simply integrating the spectrum. Instead, we replace the elastic peak by the theoretically expected,

$$I(\varepsilon) = aS(\varepsilon) = a[S'(\varepsilon) + f\delta(\varepsilon)] \tag{13}$$

then,

$$I_m(\varepsilon) = \int I(\varepsilon')R(\varepsilon - \varepsilon')\,d\varepsilon' = I'_m(\varepsilon) + afR(\varepsilon) \tag{14}$$

where $I'_m(\varepsilon)$ is the measured spectrum with the elastic peak removed, and a is the normalization factor such that $\int S(\varepsilon)\,d\varepsilon = 1$.

To find the solution of a, the sum rule of the first moment is needed. First, we multiply Eq. (5) by a, which gives

$$\langle I\rangle_1 = \int I(\varepsilon)\varepsilon\,d\varepsilon = aE_R \tag{15}$$

and obviously,

$$\langle I\rangle_0 = \int I(\varepsilon)\,d\varepsilon = a. \tag{16}$$

Then we get a pair of equations by substituting them into Eqs. (9) and (10),

$$a = \int I_m(\varepsilon)\,d\varepsilon = \int I'_m(\varepsilon)\,d\varepsilon + af\int R(\varepsilon)\,d\varepsilon$$

$$= \int I'_m(\varepsilon)\,d\varepsilon + af \tag{17}$$

$$aE_R + a\int R(\varepsilon)\varepsilon\,d\varepsilon$$

$$= \int I_m(\varepsilon)\varepsilon\,d\varepsilon$$

$$= \int I'_m(\varepsilon)\varepsilon\,d\varepsilon + af\int R(\varepsilon)\,\varepsilon\,d\varepsilon \tag{18}$$

from which a and f are solved,

$$a = \frac{1}{E_R}\int I'_m(\varepsilon)\varepsilon\,d\varepsilon - \frac{1}{E_R}\int I'_m(\varepsilon)\,d\varepsilon\int R(\varepsilon)\varepsilon\,d\varepsilon \tag{19}$$

$$f = 1 - \frac{1}{a}\int I'_m(\varepsilon)\,d\varepsilon. \tag{20}$$

With the normalized spectrum, the mean kinetic energy of the nuclei and the mean force constant experienced by the nuclei are derived by virtue of the moment sum rules (6) and (7). In this experiment, the recoilless fraction f is found to be 0.796(2), the mean kinetic energy per nucleus 42.9(3) meV, and the mean force constant $1.74(6)\times 10^8$ N/m.

Finally, if a harmonic lattice model is assumed, the inelastic part of the function $S(\varepsilon)$ can be further separated into single- and multi-phonon contributions, i.e., $S'(\varepsilon) = S'_1(\varepsilon) + S'_2(\varepsilon) + S'_3(\varepsilon) + \cdots$. In the harmonic model, phonons are treated as non-interacting particles. Multi-phonon contribution arises when more than one phonons are created or destroyed at the instant of absorption. For both isotropic [5] and anisotropic lattices [8], these terms are found to follow certain recursive relations, which makes it possible to actually calculate each term by the method of Fourier-Log decomposition [9]. It also has been shown that the (partial) phonon density of states per unit energy per atomic volume, $\mathscr{D}(\varepsilon)$, is directly related to the single phonon term [5],

$$\mathscr{D}(\varepsilon) = 3\frac{\varepsilon}{E_R}\frac{S'_1(\varepsilon)}{f}\left[1 - \exp\left(-\frac{\varepsilon}{k_B T}\right)\right]. \tag{21}$$

There is no dependence on the photon momentum $\boldsymbol{k}$ in the data analysis for α-Fe, since it has a BCC structure and is an isotropic lattice. The above-mentioned Fourier-Log decomposition is carried out to separate multi-phonon contributions and to extract the phonon density of states (DOS). Fig. 4 shows the first three terms of the multi-phonon expansion of the inelastic $S'(\varepsilon)$. It can be seen that for this sample the single phonon contribution dominates, and this can be attributed to the high recoilless fraction of 0.796. The phonon DOS for α-Fe derived from the experiment is shown in Fig. 5, compared with the calculated DOS from coherent inelastic neutron scattering

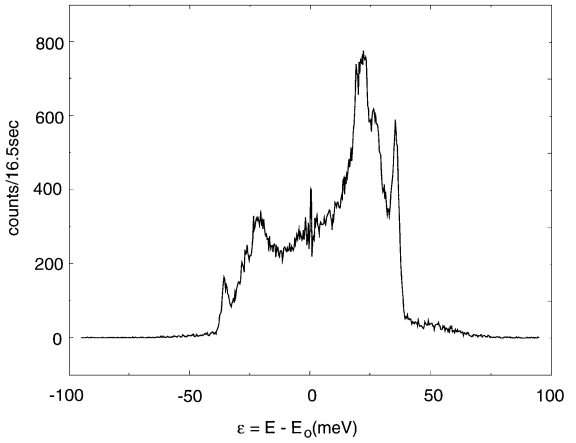

Fig. 3. The combined spectrum from 5 measured spectra with the elastic peaks removed.

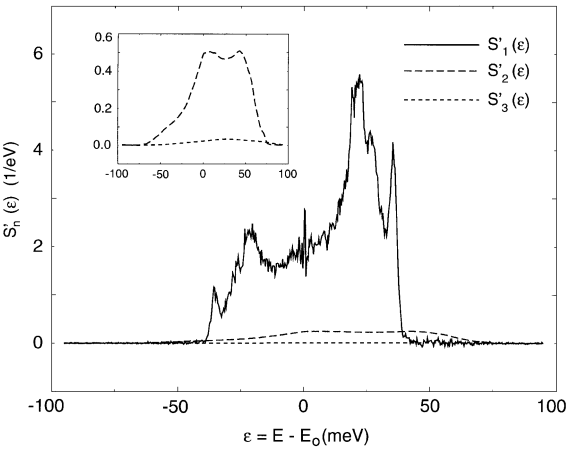

Fig. 4. The single and multiple phonon contributions to $S'(\varepsilon)$. The inset shows $S'_2(\varepsilon)$ and $S'_3(\varepsilon)$ on an enlarged scale.

data [10]. Very good agreement is evident from the figure.

We have outlined the data analysis procedure for inelastic nuclear resonant absorption experiments and demonstrated how to extract information on lattice dynamics from such experiments. We discuss this in the context of an isotropic lattice. For anisotropic lattice, there will be explicit $\boldsymbol{k}$ dependence, and the whole procedure remains the same, only the interpretations of the quantities obtained are different. For example, then obtained $f(\boldsymbol{k})$ is the Lamb-Mössbauer factor in $\boldsymbol{k}$ direction, and $\mathscr{D}(\varepsilon,\boldsymbol{k})$

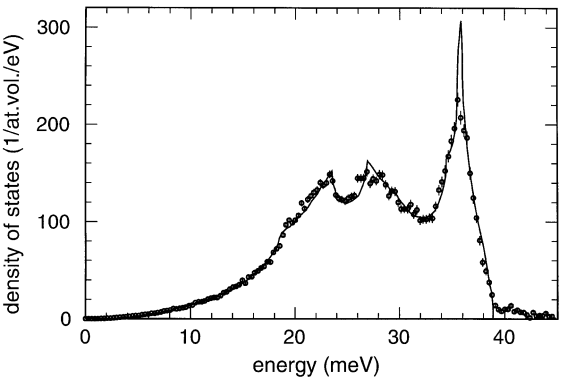

Fig. 5. The phonon DOS of α-Fe (circles), compared with that derived from the neutron data of Minkiewicz et al. [10] (solid line).

becomes projected phonon DOS [8]. This technique presents itself as a complement to other techniques currently being used in the study of vibrational dynamics. Its element selectivity is certainly unique, and the ability to be able to work with small samples and less material is advantageous.

This work was done at the SRI CAT Sector 3 undulator beamline of the Advanced Photon Source, Argonne National Laboratory, and is supported by the U.S. Department of Energy, Basic Energy Sciences, Office of Energy Research, under the contract No. W-31-109-ENG-38.

References

[1] M. Seto, Y. Yoda, S. Kikuta, X.W. Zhang, M. Ando, Phys. Rev. Lett. 74 (1995) 3828.
[2] W. Sturhahn, T.S. Toellner, E.E. Alp, X. Zhang, M. Ando, Y. Yoda, S. Kikuta, M. Seto, C.W. Kimball, B. Dabrowski, Phys. Rev. Lett. 74 (1995) 3832.
[3] T.S. Toellner, M.Y. Hu, W. Sturhahn, K. Quast, E.E. Alp, Appl. Phys. Lett. 71 (1997) 2112.
[4] W.M. Visscher, Ann. Phys. 9 (1960) 194.
[5] K.S. Singwi, A. Sjolander, Phys. Rev. 120 (1960) 1093.
[6] W. Sturhahn, T.S. Toellner, K.W. Quast, R. Röhlsberger, E.E. Alp, Nucl. Instr. and Meth. A 372 (1996) 455.
[7] H. J. Lipkin, Phys. Rev. B 52 (1995) 10 073.
[8] V.G. Kohn, A.I. Chumakov, R. Rüffer, Phys. Rev. B 58 (1998) 8437.
[9] D.W. Johnson, J.C.H. Spence, J. Phys. D 7 (1974) 771.
[10] V.J. Minkiewicz, G. Shirane, R. Nathans, Phys. Rev. 162 (1967) 528.